# A parameter study on the effect of slag electric conductivity on the solidification of a large scale ESR ingot

E. Karimi-Sibaki[1], A. Kharicha[1,2], M. Wu[1,2], A. Ludwig[2] , H. Holzgruber [3]
B. Ofner [3], M. Ramprecht [3]

[1] Christian Doppler Laboratory for Advanced Process Simulation of Solidification and Melting,
[2] Chair of Simulation and Modeling of Metallurgical Processes, Univ. of Leoben, Austria
[3] INTECO Special Melting Technologies GmbH, 8600 Bruck/Mur, Austria

**KEYWORDS:** Electroslag remelting (ESR), Magnetohydrodynamics (MHD), Solidification, Electric conductivity, Current path, Mold current, Melt pool shape.

## ABSTRACT

During the electroslag remelting process (ESR), the steel electrode is melted and re-solidified directionally in a water-cooled mold to build the high grade ingot. The quality of the ingot is governed by the solidification which is characterized by the shape of the melt pool i.e. the depth, thickness of mushy zone, and etc. The shape of the melt pool is strongly dependent on the conditions of the temperature distribution and flow which are in turn influenced by the electrical parameters such as the electric conductivity of the slag (solid and liquid). The latter dominantly controls the electric current path in the process. Here, we perform a numerical study to investigate the effect of the electric conductivity of the slag on the pool shape of a large scale ESR ingot ($\phi$ 1823 mm). For this purpose, simulations considering different current paths (with or without mold current) are performed. Some details will be analyzed in the paper.

## INTRODUCTION

The goal of the electroslag remelting (ESR) process is purifying steel or other alloys such as Ni-based super alloys. The supplied thermal energy through the Joule heating released in the slag causes formation of droplets at the tip of the remelting electrode. The droplets then pass through the slag and reach the liquid melt pool. The melt pool solidifies directionally in a water-cooled mold to manufacture the high quality ingot [1].

Most conventional ESR slags contain $CaF_2$-$CaO$-$Al_2O_3$ in which the electric current is conducted by ions [2-3]. A number of oxides such as $SiO_2$, MgO, and TiO2 may be added to modify the electric conductivity or chemical reactivity of the slag [4]. A high degree of desulphurization and deoxidation is a desirable characteristic of the slag [5]. Additionally, the electrical conductivity of slag must be decreased to generate sufficient heat through the Joule heating.

In fact, the flow of the molten slag and liquid melt pool is strongly influenced by the electromagnetic field in the ESR process. Consequently, the electrical parameters such as the AC frequency and electric conductivity of the slag have a significant effect on the quality of the final ingot. Principally, the current path is strongly dependent on the electric conductivity of slag (liquid and solid). In spite of low electric conductivity of the solid slag skin, considerable amount of current can cross the solid slag skin (mold current) entering into the mold [6-8]. In the current

INDEX

work, the influence of the electric conductivity of the slag on the pool shape of a large scale ESR ingot is numerically investigated.

## A BREIF DESCRIPTION OF MODEL

The electromagnetic field, fluid flow, heat transfer, and solidification during the ESR process are modeled using the Finite Volume Method (FVM). The equations are implemented in the commercial CFD software, FLUENT-ANSYS v.14.5, using User-defined functions (UDF). An axisymmetric computational domain is considered for our simulations as illustrated in Fig. 1. The crystal morphology is assumed to be mainly columnar and dendritic, thus the mushy zone is considered as a porous media. The interdendritic flow in the mushy zone is modelled based on the permeability law of Black-Kozeny [9].

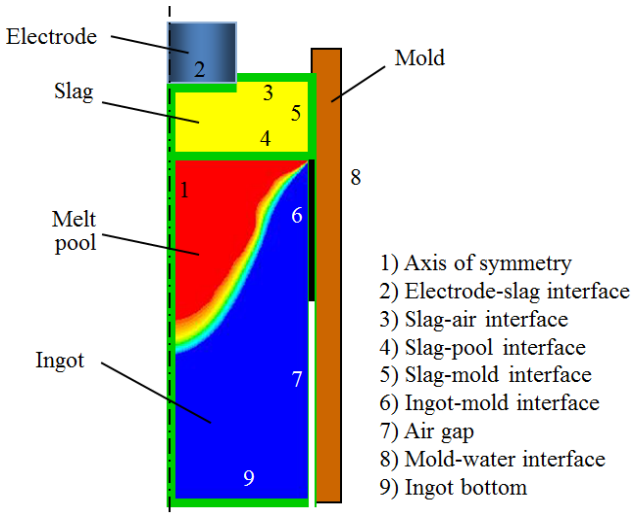


Fig. 1. Schematic representation of the boundaries and computational domain.

The Phasor notation can be used to express the sinusoidal AC magnetic field in the process ($B_\theta = \tilde{B}_\theta e^{i\omega t}$) where ω is the angular frequency. The equation to be solved is given as:

$$\frac{\partial B_\theta}{\partial t} + \left[ \frac{\partial}{\partial z}\left( \frac{1}{\sigma \mu_0} \frac{\partial B_\theta}{\partial z} \right) + \frac{\partial}{\partial r}\left( \frac{1}{r \sigma \mu_0} \frac{\partial (r B_\theta)}{\partial r} \right) \right] = 0 \qquad (1)$$

Where $\mu_0$ and σ are magnetic permeability and electric conductivity of the materials. The boundary conditions for Eq. (1) are obtained using the Ampere's law. The magnitude of magnetic flux is prescribed at mold-water and slag-air interfaces. In addition, the continuity of magnetic induction is applied at slag-pool, slag-mold and ingot-mold interfaces. After computing the magnetic field, the electric current can be obtained through: $\tilde{\vec{j}} = \frac{1}{\mu_0}(\vec{\nabla} \times \tilde{B}_\theta)$ . Finally, the time averaged Lorentz force ($\vec{F}_L$) and Joule heating ($q_{Joule}$) can be calculated:

INDEX

$$\vec{F}_L = \mathrm{Re}\left(\frac{1}{2}\vec{j} \times \tilde{B}_{\theta\ Conjugate}\right) \quad (2)$$

$$q_{Joule} = \mathrm{Re}\left(\frac{1}{2\sigma}\tilde{\vec{j}} \times \tilde{\vec{j}}_{\theta\ Conjugate}\right) \quad (3)$$

The Lorentz force and Joule heating are added as source terms to momentum and energy equations respectively. More details about the solution of induction equation and the required boundary conditions for ESR process were presented by Kharicha [10].
The slag-pool, slag-air, and electrode-slag interfaces are assumed to be stationary and flat. Moreover, the immersion depth of the electrode is ignored in this study. The flow and thermal boundary conditions refer to the previous publication [11]. The thickness of solidified slag layer is estimated based on plant observation to be 1 cm. The slag skin layer is not in full contact with the mold surface due to shrinkage of the solidified ingot and subsequent formation of an air gap. As such, a value of 5 cm is estimated for the length of the contact region between the ingot and mold. The average physical properties of the steel and slag, operation conditions, and process geometry are listed in Table 1.

Table 1. Parameters used for our simulations.

| **Slag** | |
|---|---|
| Density ($kg \cdot m^{-3}$) | 2800 |
| Viscosity ($Kg \cdot m^{-1} \cdot s^{-1}$) | 0.002 |
| Specific heat, liquid ($J \cdot Kg^{-1} \cdot K^{-1}$) | 1250 |
| Thermal Conductivity, liquid($W \cdot m^{-1} \cdot K^{-1}$) | 10 |
| **Steel** | |
| Density ($kg \cdot m^{-3}$) | 7100 |
| Viscosity ($Kg \cdot m^{-1} \cdot s^{-1}$) | 0.006 |
| Liquidus Temp. (K) | 1779 |
| Solidus Temp. (K) | 1719 |
| Specific heat, liquid ($J \cdot Kg^{-1} \cdot K^{-1}$) | 800 |
| Latent heat of fusion ($J \cdot Kg^{-1}$) | 268000 |
| Thermal Conductivity, liquid($W \cdot m^{-1} \cdot K^{-1}$) | 40 |
| Electric Conductivity, liquid($ohm^{-1} \cdot m^{-1}$) | 880000 |
| **Operation conditions** | |
| RMS current (kA) | 36.5 |
| AC frequency (Hz) | 0.2 |
| Power (MW) | 1.8 |
| **Geometry (Static mold)** | |
| Mold radius (m) | 0.9115 |
| Electrode radius (m) | 0.725 |
| Slag height (m) | 0.265 |

The slag system designed for this process has approximately the following composition ($CaF_2$: 30-40%, CaO: 30-40%, $Al_2O_3$: 30-40%). The electric conductivity of this slag in liquid phase was reported [12] to be between 80-300 $\Omega^{-1}.m^{-1}$. However, the parameter is unknown for the slag in solid phase. The slag skin layer is assumed to be a perfect electrical insulator in most of

simulations found in literature. On the other hand, preliminary trials to produce ESR ingot using the current conductive mold (CCM) technology strongly rejects this assumption [13]. Furthermore, the perfect contact between the mold and baseplate brings the possibility for a portion of current to go directly toward the mold. In fact, the current selects the less resistive path through either the mold or melt pool to reach the baseplate. In the current study, the amount of power generated in the process is known in advance. This provides us helpful information to theoretically analyze the amount and consequences of mold current in the ESR process.

## RESULTS AND DISCUSSIONS

A number of simulations were performed to compute the electric current path and total power consumption in the process considering variable magnitude for electric conductivity of slag and solidified slag skin. The target power of the process is known and given in Table 1. For this reason, the conductivity of slag skin layer is tuned to generate the target power in the system. In other words, variation in total power consumption as a function of slag skin electric conductivity was calculated whereas the conductivity of liquid slag is kept constant. The aim is to estimate adequate values of electric conductivity for the slag and solidified slag layer. As indicated in Fig. 2, a summary of the results is plotted where each curve is obtained for a constant electric conductivity of liquid slag. The calculated power decreases almost exponentially with the increase of slag skin electric conductivity. The latter indicates that opening the path to the mold decreases the overall resistance of the whole system.

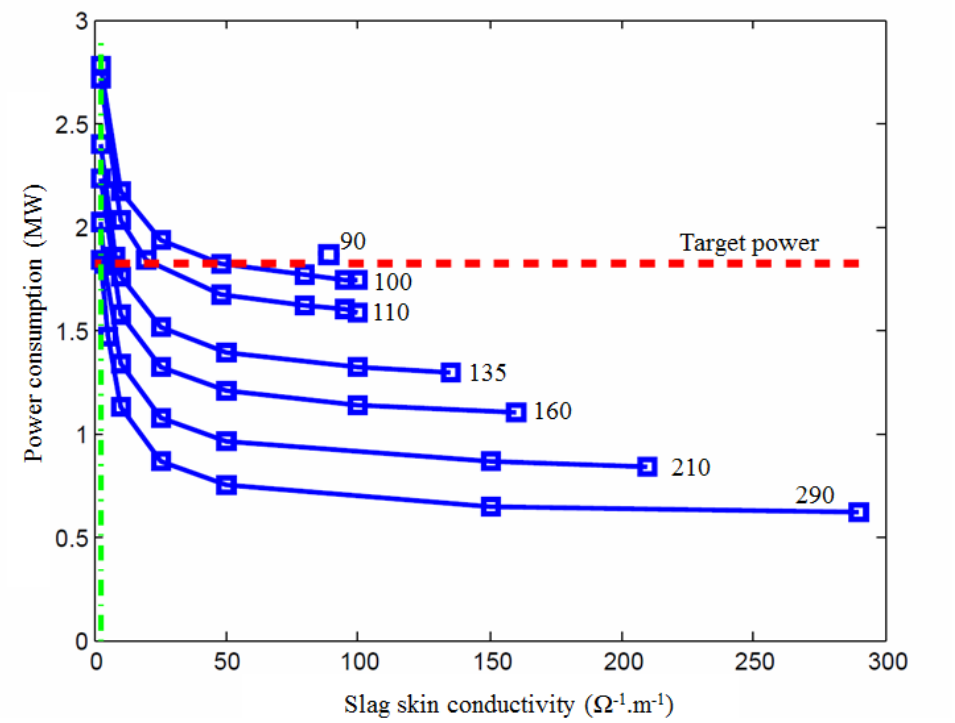


Fig. 2. Total power consumed in the process versus the electric conductivity of solidified slag layer (the constant value used to label each curve indicates the conductivity of liquid slag.)

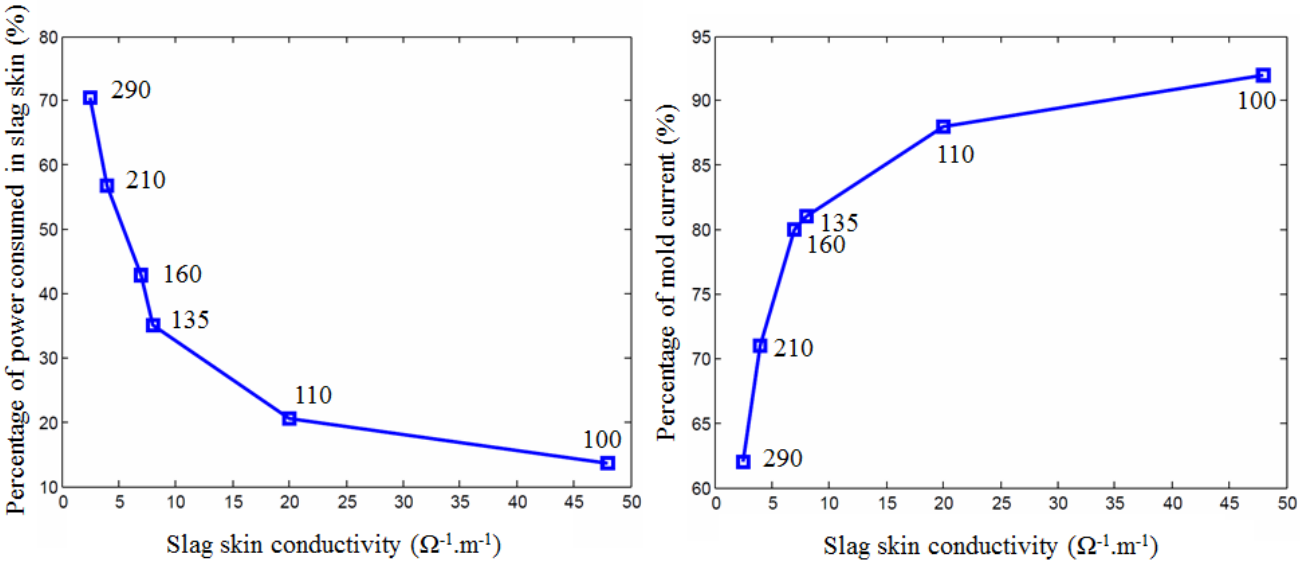


(a) (b)

Fig. 3. Proportion of (a) total power consumed in slag skin, (b) electric current entering into the mold, at target power, (the points are labeled according to the conductivity of liquid slag).

Since the target power is known, some correlations can be established between the electric conductivities of slag (liquid and solid), proportion of mold current, and proportion of total power consumed in solid slag layer. For the adequate conductivities, the amount of mold current and fraction of total power consumed in the slag skin were computed. The analyses were plotted against the conductivity of solid slag skin as shown in Fig. 3. The proportion of generated power in slag skin layer is raised by decrease of electric conductivity as indicated in Fig. 3 (a). The results reveal that significant amount of Joule heating is released in the thin layer of slag skin. For this reason, the skin layer will be definitely remelted and assumption of constant thickness is not valid. However, the generated power in solid slag layer with electric conductivity of 48 is negligible compared to the total consumed power in the system (~ 12% of total power). Accordingly, our primary assumption of constant thickness of the skin layer can be accepted for this case. For the latter, the ratio of current entering into the mold was predicted to be around 92 % as shown in Fig. 3 (b).

In order to explore the influence of mold current on the formation of solidifying ingot, we continue our study for two extreme cases in which the fundamental assumptions (e.g. constant thickness of slag skin layer) are valid. The operation conditions of the case studies are listed in Table 2.

Table 2. Operation conditions of the case studies.

| | Electric conductivity of liquid slag ($ohm^{-1}\cdot m^{-1}$) | Electric conductivity of solid slag skin ($ohm^{-1}\cdot m^{-1}$) | Mold current |
|---|---|---|---|
| Case I | 100 | 48 | YES |
| Case II | 90 | Perfect insulator | NO |

The current paths in the whole system are compared for the two cases (with and without mold current) as shown in Fig. 4. In the case with mold current, a significant portion of current enters

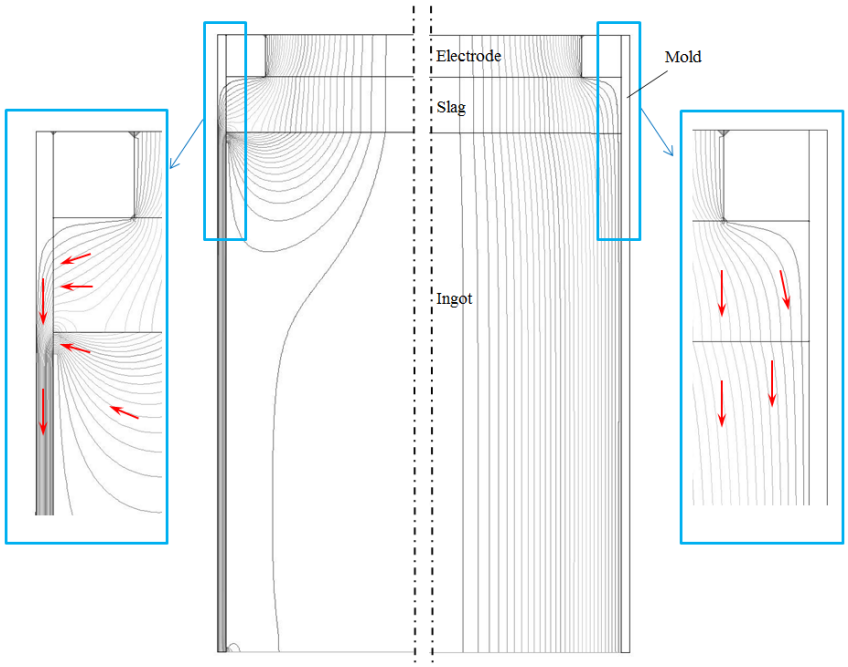


Fig. 4. Comparison of electric current paths (red arrows show the direction of current path) between the cases of (a) conducting slag skin, and (b) insulating slag skin.

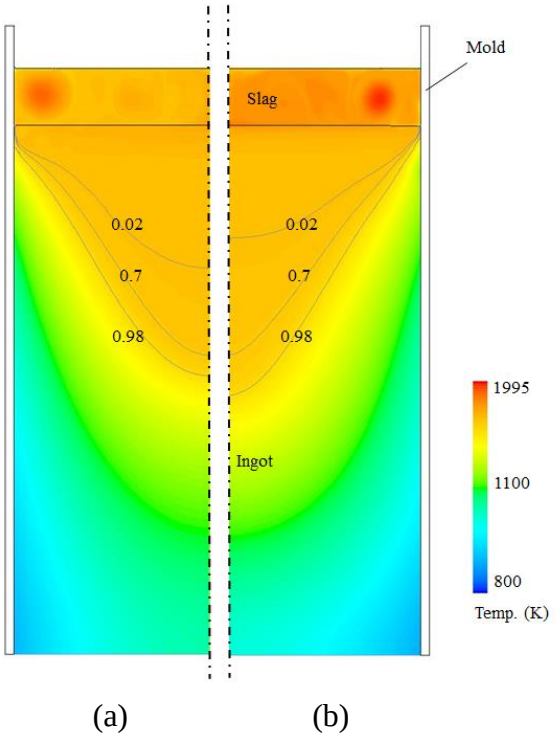


Fig. 5. Contour of temperature overlaid with isolines of fraction solid (0.02, 0.7, 0.98) to indicate the mushy zone, (a) with mold current, (b) without mold current.

INDEX

to the mold from the contact region where noticed to be the most favorable path with minimum electrical resistance. In addition, the temperature field and pool shape are compared as shown in Fig. 5. In fact, mold current intensifies stirring leads to approximately uniform temperature in slag and melt pool regions. In the case with mold current, the depth of melt pool (the distance between the slag-pool interface and the isoline of 0.02 solid fraction) is increased. As a matter of fact, promotion of stirring with mold current enhances the global energy transfer in the process results in deeper pool and thinner mushy zone. Additionally, the distance from the slag-pool interface to the start of solidification at the ingot surface known as standing height (liquid cap) is increased. With mold current, the direction of Lorentz force bents downward near the contact region. Consequently, the hot liquid metal is pushed down near the mold wall causes increase of standing height.

## SUMMARY

A numerical study was performed to investigate the influence of electric conductivity of slag (liquid and solid) on the shape of the melt pool for a large scale ESR ingot (ϕ 1823 mm). The electric current path lines were computed in the whole system considering variable electric conductivity for liquid slag and solidified slag layer. Some correlations between the conductivities are established according to the total power generated in slag and solidified slag skin. It is found that a significant amount of current can flow through the mold (mold current) despite low electric conductivity of slag skin layer. Furthermore, the fraction of mold current is increased exponentially by the decrease of electric conductivity of liquid slag. Additionally, two extreme cases are compared (with and without mold current) concerning the effect of mold current on the pool shape. Essentially, the mold current can significantly influence the standing height (liquid cap) and the melt pool shape by promoting stirring in the process. The standing height is increased and the melt pool becomes deeper in the case with mold current.

## ACKNOWLEDGEMENTS

The authors acknowledge the financial support by INTECO GmbH and the Austrian Federal Ministry of Economy, Family and Youth and the National Foundation for Research, Technology and Development within the framework of the Christian Doppler Laboratory for Advanced Process Simulation of Solidification and Melting.

## REFERENCES

[1] G. Hoyle, Electroslag Processes, Applied Science Publishers, London (1983).
[2] A. Mitchell and G. Beynon, Met. Trans B. 10, (1971), p.3333.
[3] M.E. Peover, J. Inst. Metals. 100, (1972), p.97.
[4] K. Wroblewski, J. Fraley, J. Fields, R. Ewerner, S. Rudoler, Proc. of LMPC, Nancy (2011), p.121.
[5] J.J. Debarbadilo , Met. Trans A. 14, (1983), p.329.
[6] A. Kharicha, E. Karimi Sibaki, M. Wu, A. Ludwig, Proc. of LMPC, Texas (2013), p.95.

INDEX

[7] M. Kawakami, K. Nagata, M. Yamamura, N. Sakata, Y. Miyashita, and K.S. Goto, Testsu-to-Hagane, 63 (1977), p. 220.
[8] S.F. Medina and M.P. de Andres, Ironmaking and steelmaking, 14 (3) (1987), p.110-121.
[9] V. R. Voller, and C. Prakash, Int. J. Heat Mass Transfer, 30(8), (1987), p.1709.
[10] A. Kharicha, W. Schützenhöfer, A. Ludwig, and R. Tanzer, Proc. of LMPC, Nancy (2011), p.113.
[11] E. Karimi-Sibaki, A. Kharicha, M. Wu, A. Ludwig, et al., Proc. of LMPC, Texas (2013), p.13.
[12] M.hajduk and T.E. Gammal, Stahl Eisen, 99 , (1979), p.113.
[13] H. Holzgruber, W. Holzgruber, A. Scheriau, et al., Proc. of LMPC, Nancy (2011), p.57.

INDEX